



HAL
open science

Fourier-like conduction and finite one-dimensional thermal conductivity in long silicon nanowires by approach-to-equilibrium molecular dynamics

Hayat Zaoui, Pier Luca Palla, Fabrizio Cleri, Évelyne Martin

► To cite this version:

Hayat Zaoui, Pier Luca Palla, Fabrizio Cleri, Évelyne Martin. Fourier-like conduction and finite one-dimensional thermal conductivity in long silicon nanowires by approach-to-equilibrium molecular dynamics. *Physical Review B*, 2017, 95 (10), 104309, 7 p. 10.1103/PhysRevB.95.104309. hal-03407494

HAL Id: hal-03407494

<https://hal.science/hal-03407494>

Submitted on 18 Jan 2022

HAL is a multi-disciplinary open access archive for the deposit and dissemination of scientific research documents, whether they are published or not. The documents may come from teaching and research institutions in France or abroad, or from public or private research centers.

L'archive ouverte pluridisciplinaire **HAL**, est destinée au dépôt et à la diffusion de documents scientifiques de niveau recherche, publiés ou non, émanant des établissements d'enseignement et de recherche français ou étrangers, des laboratoires publics ou privés.

Fourier-like conduction and finite 1D thermal conductivity in long silicon nanowires by approach-to-equilibrium molecular dynamics

Hayat ZAOUI, Pier Luca PALLA, Fabrizio CLERI and Evelyne LAMPIN *

*Institut d'Electronique,
Microelectronique et de Nanotechnologies,
F-59000 Lille, France*

Abstract

The thermal conductivity of cylindrical and smooth silicon nanowires is systematically studied as a function of diameter and length by fully-atomistic simulations. A transient thermal regime is created and monitored by molecular dynamics. This approach-to-equilibrium methodology, already proven to be very efficient for bulk systems, is systematically applied to nanowires of lengths up to 1.2 micron, and diameters in the range 1 to 14 nm. It is shown that the temperature profile along the nanowire axis and its temporal evolution comply with the heat equation. A 1D thermal conductivity is extracted from the characteristic decay time according to the time-dependent solution of the heat equation. Like in bulk using the same method, the thermal conductivity exhibits a length dependence due to the accumulation of the phonon mean free paths distribution. Unlike in bulk, the saturation is observed, due to a reduction of the phonon mean free paths estimated to hundred or nanometers. A finite thermal conductivity can be extracted for each diameter, and a divergence at long length is not observed.

* evelyne.lampin@univ-lille1.fr

I. INTRODUCTION

The thermal conductivity of silicon nanowires (NWs) 115 to 22 nm in diameters and micrometer long has been measured more than 10 years ago.¹ At room temperature, it decreases from about $150 \text{ W.K}^{-1}.\text{m}^{-1}$ in bulk silicon² to about $10 \text{ W.K}^{-1}.\text{m}^{-1}$ in the thinnest NWs. Such a drop in thermal conductivity has opened up a wide interest for thermoelectricity, a major improvement in the figure of merit of thermoelectric converters being expected provided that a high value of electrical conductivity can be preserved. Still a controversy remains whether the heat transport behaves or not according to the Fourier law. This controversy is fed by the length dependence of the thermal conductivity. Experimentally, it is extremely challenging to measure the spatial distribution of temperature and heat flow at the nanoscale. This challenge becomes ever dramatic when very thin NWs are targeted, such as the sub-10 nm NWs used in the most advanced nanoelectronic technologies. The problem has been however addressed on other 1D systems : carbon and boron nitride nanotubes³ and SiGe nanowires⁴. The thermal conductivity presents a dependence even for lengths L longer than the average phonon mean free path (MFP) l_{ph} that one can extract from the bulk thermal conductivity κ_{bulk} using the kinetic theory (C is the heat capacity and v the sound velocity):

$$\kappa_{\text{bulk}} = \frac{1}{3} C v l_{\text{ph}} \quad (1)$$

i. e. around 50 nm for Si at room temperature. A length dependence of Si NWs thermal conductivity is also obtained by atomic scale simulations⁸⁻¹⁰ using the direct method⁵ give a length dependence of the thermal conductivity of silicon nanowires⁸⁻¹⁰. At short length, a first regime shows a pronounced length dependence, which is attributed to a ballistic regime for $L < l_{\text{ph}}$ ⁸⁻¹⁰. It must be emphasized that a length dependence is also obtained using the same method when bulk Si is studied⁵. At long length, the calculations by Hu¹⁰ saturate to a constant thermal conductivity while N. Yang⁸ and X. Yang⁹ obtain a divergence of κ versus L .

The length dependence of the thermal conductivity is not directly related to a violation of the Fourier law nor to a ballistic regime. Indeed, the length dependence is also observed in atomistic simulations on bulk silicon. Recently, it has been shown^{6,7} that the phonon MFPs are distributed on several orders of magnitude, and reach 10 μm in bulk silicon. The average value approximated by the above kinetic theory can not therefore be a criterium

of saturation of the thermal conductivity. Until the system length has not reached the maximum phonon MFP, the contributions of the latter progressively accumulate and result in a length dependence. Though, several questions remain open related to the width of the phonon MFPs distribution in Si NWs and to a possible deviation from the diffuse regime described by the Fourier law. In the present work, we adress these issues by a systematic study of the thermal conductivity dependence on the Si NWs diameter and length. The latter have been pushed up thanks to a very efficient atomistic MD method for the simulation of thermal properties that we recently developed:^{11,12} the Approach-to-Equilibrium MD (AEMD). The speed up is due to the exploitation of heat transients, rather than the stationary regime common to other MD-based approaches. A length dependence is observed, as in the direct method. Its origin has been clearly explained¹³ and its correlation with the phonon MFP distribution has been demonstrated. The methodology, recalled in the next section, is used to answer the following questions : does the temperature profile and evolution comply to the heat equation (i.e. Fourier-like) ? Is the thermal conductivity finite or not at long length ? What is the evolution of the thermal conductivity as a function of the diameter ? And finally what can we learn on the phonon MFP distribution in the nanowire ?

II. ATOMISTIC METHOD

Smooth-surface NWs are obtained by cutting a cylinder of diameter D and length L from a silicon block with diamond-lattice atomic structure (Fig. 1). The circular section is preferred to the square one since it is closer to the real shape of Si NWs usually fabricated from either the top-down or bottom-up technologies^{14,15}. The interactions between silicon atoms are modeled using the Tersoff interatomic potential¹⁶. The lattice parameter is taken equal to that of bulk crystalline Si for this potential scheme, $a_0=5.45 \text{ \AA}$ at 500 K. The axis of the nanowire is along the [001] direction (noted z). The diameter D is varied from 1 nm for the thinnest wires to 14 nm for the largest. Periodic boundary conditions are applied along the z -direction.

The Approach-to-Equilibrium Molecular Dynamics method is used to create and monitor a temperature transient, by looking at the decay time of a temperature difference ΔT to obtain the NW thermal conductivity. Two Nosé-Hoover thermostats are used to split the

NW into a cold block at temperature $T_1 = 400$ K for $0 < z < L/2$, and a hot block at temperature $T_2 = 600$ K for $L/2 < z < L$. Due to the presence of the surface, the thermalisation of the hot/cold blocks could be slower compared to the bulk case but we checked that the duration of the constant $\{NVT\}$ MD simulation can be maintained within the range 100 ps to 1 ns without impacting the final result. Therefore we most often take 100 ps, to further minimize the computational cost. After the thermalization phase the two thermostats are switched off, and the system is left free to reach thermal equilibrium at constant $\{NVE\}$. During the approach-to-equilibrium, the temperature difference ΔT between the two blocks is followed up. It can be seen from the semi-log plot in Fig. 2 that ΔT tends to 0 with an exponential decay, i. e. the same behaviour already observed in bulk materials^{11,12}. The final temperature of the nanowire is equal to 500 K, therefore quantum effects, which are not described by classical MD simulations, should not be relevant (Debye temperature of silicon = 645 K).

A fine determination of the decay time τ is made for each decay curve. Many exponential fits are performed with an incremental initial time to extract the mean value and error, and to remove the initial fast transient corresponding to the switching from $\{NVT\}$ to $\{NVE\}$. In this way, we recover only the intrinsic thermal decay time. In addition, averaging is performed over a couple of simulations for the smallest sizes more sensitive to the particular set of initial atomic velocities determined randomly following a Maxwell-Boltzmann distribution.

III. TRANSIENT ANALYSIS AND 1D THERMAL CONDUCTIVITY

The nanowires studied by molecular dynamics have a finite section by construction. Therefore, the thermal current does not need to be normalized by unit section to be a finite quantity as in the case of a bulk or by unit length as in the case of a plane like graphene. The 1D formulation of the Fourier law then gives:

$$\vec{\varphi}(W) = -\kappa_{1D}(W.m.K^{-1})\vec{\text{grad}}T(K) \quad (2)$$

where $\vec{\varphi}$ is the thermal current and κ_{1D} is a 1D thermal conductivity.

We now derive the 1D heat equation in the nanowire. The nanowire supercell unit of length L with periodic conditions along z that we study by molecular dynamics is schema-

tized in Fig. 3. The amount of heat δQ supplied to this unit between t and $t + dt$ is equal to:

$$\delta Q = (\varphi_i - \varphi_o) dt \quad (3)$$

where φ_i and φ_o are the inward and outward thermal currents. The change in enthalpy dH of this unit between the same time interval is equal to:

$$dH = \frac{\partial}{\partial t} \left(\int_0^L \rho C T dz \right) dt \quad (4)$$

with C the heat capacity ($J.K^{-1}$) and ρ the number 1D density in m^{-1} . As in the derivation of the heat equation in 3D, the time derivative can be displaced inside the integral where it applies to T only:

$$dH = \left(\int_0^L \rho C \frac{\partial T}{\partial t} dz \right) dt \quad (5)$$

On the other hand, δQ can be rewritten using an integral over z :

$$\delta Q = - \left(\int_0^L \frac{\partial \varphi}{\partial z} dz \right) dt = - \left(\int_0^L \kappa_{1D} \frac{d^2 T}{dz^2} dz \right) dt \quad (6)$$

According to the first thermodynamics law, the two quantities dH and δQ are equal and we obtain the 1D heat equation:

$$\frac{\partial T}{\partial t} = \frac{\kappa_{1D} \cdot L}{3Nk_B} \frac{\partial^2 T}{\partial z^2} \quad (7)$$

where the Dulong and Petit law has been assumed for the heat capacity. This equation can be solved as in the bulk case¹⁷ and the solution is a Fourier series with a dominant contribution :

$$T(t, z) = \frac{1}{2}(T_1 + T_2) + \frac{2}{\pi}(T_2 - T_1) \sin \left(\frac{2\pi}{L} z \right) \times e^{-t/\tau} \quad (8)$$

where

$$\tau = \frac{3Nk_B L}{4\pi^2} \frac{1}{\kappa_{1D}} \quad (9)$$

The temperature difference during the approach-to-equilibrium is a sum of decaying exponentials:

$$\Delta T(t) = \sum_{m=0}^{\infty} \frac{8(T_2 - T_1)}{(2m+1)^2 \pi^2} e^{-(2m+1)^2 t/\tau} \quad (10)$$

This expression tends to a single exponential decay for long times that corresponds to the major contribution for $m = 0$. The decay time extracted by the procedure presented in the previous part corresponds to this contribution, and can therefore be used to obtain the 1D thermal conductivity following:

$$\kappa_{1D} = \frac{3Nk_B L}{4\pi^2} \frac{1}{\tau} \quad (11)$$

The NW 1D thermal conductivities are plotted versus length in Fig. 4, for diameters ranging from 1 to 14 nm. The speed up provided by the exploitation of the transient regime allowed us to study diameter and lengths that far exceed previous simulations⁸⁻¹⁰. The number of atoms in the biggest systems ($D=14$ nm and $L = 1.2 \mu\text{m}$) exceeds 9 millions. The thermal conductivities strongly depend on the NW length. A length dependence has also been observed when we apply the same methodology to bulk systems and was attributed to a progressive accumulation of the contributions of the largest phonon MFPs when the length of the simulation supercell increases.¹³ The length dependence in the NWs and the consequences for the phonon MFPs will be discussed in the following sections.

IV. CONDUCTION REGIME IN THE NANOWIRES

In the range of lengths where the NWs thermal conductivity varies, an open question is whether the Fourier regime is valid, and therefore whether the temperature profile along z and the temporal evolution of the temperature difference between the hot and cold blocks still agree with Eqs. 8 and 10. We have investigated this point in the case of the thicker NW, because the temperature fluctuations will be the smallest among the family of NWs studied due to an average on a larger number of atoms in a slice. We have looked into details to three supercell lengths : a long length (600 nm) in the plateau of the $\kappa(L)$ curve, and two small lengths in the region of strong variation of κ : 75 and 150 nm. For these 3 lengths, the temperature difference behaves exponentially at long time as evidenced by the red lines superimposed on the MD evolution in Fig. 5. However, a small deviation from the exponential decay exists at the beginning of the approach-to-equilibrium, and can be seen in the figure for the longest wire before 50 ps. As discussed in the previous part, it is due to the switching from {NVT} to {NVE}. We have followed up the temperature profile in intervals far away from this initial transient, at times where only the Fourier regime should be accounted for. The intervals are indicated by arrows in Fig. 5 for each size. In these intervals, the temperature difference is around 100 K. The temperature profiles averaged on these intervals are presented in Fig. 6. The temperature profiles are presented on the same z scale, they are repeated according to the periodic boundary conditions for the two smaller lengths. The MD results in black are sine function of the form $T(z) = T_m + \Delta T \sin(2\pi z/L)$ as evidenced by the superimposing of the red curves obtained by adjusting only T_m and ΔT .

The temperature profiles are therefore of the form obtained in Eq. 8 by solving the heat equation, even for the smallest length in the domain where the dependence of the thermal conductivity with the length is significant. In conclusion, both the temporal evolution of the temperature difference of the hot and cold blocks, and the temperature profile along the nanowire length do agree with the heat equation. We are therefore in a Fourier regime even if the thermal conductivity is not that of bulk silicon, and does vary with the supercell length.

V. THERMAL CONDUCTIVITY AT LONG LENGTH

A. Does the conductivity diverge ?

In the literature, the thermal conductivity of the nanowires computed by MD is found to saturate at long length by Hu et al.¹⁰ while it diverges in the studies by N. Yang et al⁸ and X. Yang et al⁹. In these three works, the direct method is used to obtain the thermal conductivity of square-section nanowires. The same interatomic potential by Stillinger and Weber²⁷ is used, and the calculations are performed at room temperature, and up to 1000 K in the works of N. Yang and X. Yang. The thermal conductivities that we obtained by AEMD do not present any divergence when the NW length increases. In particular, Fig. 7 focuses on the $D=2$ nm nanowire studied in this work, one of our nanowire with the highest aspect ratio, up to 250. For lengths greater than 200-250 nm, the thermal conductivity remains constant. The error bar increases for the two longest NWs with $L=400$ and 500 nm due to a progressive self-heating at long time that prevents the whole temporal evolution of the temperature difference to be valuable for the determination of the decay time. This self-heating is reduced when the initial temperature difference is reduced for example to 100 K.¹⁸ It could be due to a long-time surface relaxation. The nanowire studied in Fig. 7 has a cross section comparable to the NWs studied by N. Yang and X. Yang. X. Yang obtained a thermal conductivity at $L=400$ nm twofold the thermal conductivity at $L=200$ nm, while N. Yang observed a twofold increase of the thermal conductivity from $L=200$ and $L=1000$ nm. It has been checked that the temperature effects are not at the origin of such a difference, since our calculations also saturate at 300 and 1000 K for the same diameter. The origin of the divergence is unclear, and its very existence appears quite doubtful. It must be noticed

however that is possible to extract finite thermal conductivities from experiments.¹

B. Comparison with the literature

The length dependence is an effect of the present MD method, and since our calculations converge to a finite thermal conductivity at long length, the relevant value is the thermal conductivity that corresponds to a nanowire of a given diameter but infinite length. These values are presented in Fig. 8. As a matter of comparison with bulk thermal conductivities or bulk-like determination of nanowire thermal conductivities, it is possible to obtain a pseudo 3D-thermal conductivity κ by dividing the 1D thermal conductivity by the nanowire section S :

$$\kappa_{3D}(\text{W.m}^{-1}.\text{K}^{-1}) = \frac{\kappa_{1D}(\text{W.m.K}^{-1})}{S(\text{m}^2)} \quad (12)$$

The variation range is smaller for κ_{3D} than for κ_{1D} since the smaller the section, the smaller the 1D thermal conductivity, as can be seen in Fig. 8 where the 3D thermal conductivities obtained from our 1D values are plotted in blue. It may explain, at least in part, the quasi absence of variation from $D=2$ nm to 15 nm in the EMD results.^{28,29} At $D=1$ nm however, the increase of thermal conductivity is not obtained in our approach. In these NWs, the number of atoms by plane is only equal to 4, or in other words the core of the NWs is nearly nonexistent and the inconsistencies in the system are not relevant. The 3D thermal conductivities obtained from our 1D values range from $\kappa_{3D}= 3.5 \text{ W.m}^{-1}.\text{K}^{-1}$ for $D=1\text{nm}$ and $28 \text{ W.m}^{-1}.\text{K}^{-1}$ for $D=14\text{nm}$. The reduction compared to a silicon bulk described in the same conditions (AEMD, Tersoff potential, 500K, i. e. $\kappa_{\text{bulk}}=145\pm 2 \text{ W.m}^{-1}.\text{K}^{-1}$) is ≈ 40 for $D=1\text{nm}$ and ≈ 5 for $D=14\text{nm}$. It is not possible to compare these values to experiments. Indeed although typical NW diameters of 10-15 nm are used in NW-FETs,^{14,19-22} and that ultra-thin NWs with diameters in the [3-5] nm-range^{23,24} were successfully fabricated in the most advanced technologies, the thermal conductivity has been measured only for NW diameters greater than 22 nm.¹ Concerning the modeling, Zou and Balandin²⁵ solve the Boltzman transport equation by accounting for the confinement effects on the phonon dispersion curve. They determine the dependence of the thermal conductivity on the nature of the reflection at the surface, from specular to diffuse. In molecular dynamics, both confinement and surface effects are implicitly accounted for. Our values are considerably smaller than their result in the specular case, that would a priori be more adapted to the smooth nanowires studied in

the present work. However the maximum diameter we were able to study is smaller than the case they studied ($D=20\text{nm}$), and a decrease of the thermal conductivity is expected when the diameter decreases. An additional comparison element could be obtained thanks to the determination by molecular dynamics of the impact of the surface roughness, but is outside the frame of the present work. Concerning atomistic calculations, a large part of the results published in the literature have been performed on square-section NWs. Differences are expected between circular and square sections due to the presence of edges. Moreover, it is not clear whether the results should be compared at a given cross section or at a given characteristic length (diameter or side). A strict comparison will therefore be restricted to calculations of NWs with a circular shape. The work of Ponomareva et al.²⁶ is dedicated to circular NWs oriented along the [111] direction. Although they use a different interatomic potential, the Stillinger-Weber²⁷, known to give higher thermal conductivity for bulk Si¹³, their value of $17 \text{ W.m}^{-1}.\text{K}^{-1}$ for $D=4.2 \text{ nm}$ gives a 1D thermal conductivity of $2 \times 10^{-14} \text{ W.m}^{-1}.\text{K}^{-1}$ is in agreement with our results (Fig. 8). The thermal conductivity reduction of 3-4 obtained by He and Galli²⁹ by EMD and Tersoff potential in a cylindrical NW is obtained at room temperature. We have applied the ratio to the bulk thermal conductivity at 500 K and converted the value to a 1D thermal conductivity ($\kappa_{1D}=7 \times 10^{-14} \text{ W.m}^{-1}.\text{K}^{-1}$). This point for $D=15 \text{ nm}$ is plotted in Fig. 8 and is in agreement with our calculations.

VI. PHONON MEAN FREE PATHS IN THE NANOWIRES

We have recently demonstrated¹³ that the length dependence observed in the AEMD method is due to a cutoff at L of the phonon MFPs distribution. When increasing L , the thermal conductivity increases until a threshold length (L_{th}) is reached. Above L_{th} , the thermal conductivity is constant and results from the whole distribution of phonons MFPs in the supercell unit. The value of L_{th} corresponds to the upper limit of the phonon MFP distribution in the material Λ_{max} . The curves $\kappa_{1D} = f(L)$ plotted in Fig. 4 are used to obtain the value of Λ_{max} as a function of the NW diameter (Fig. 9). The maximum phonon MFPs are in the range [100-800] nm for the diameters under study. These values are smaller than in bulk silicon : using the same methodology, we were not able to reach the saturation of the $\kappa(L)$ curve even for the largest supercell at $L=1.2 \mu\text{m}$. Other calculations in the literature^{6,7} show that the mean free path distribution extends up to $10 \mu\text{m}$ in bulk silicon.

The MFPs, although drastically lower than in bulk silicon, still remain large, hundred of times the NW diameter. This could mean that a way to improve the dissipation of self-heating in NW-based devices would be to preserve these long phonon MFPs for example thanks to a surface state as smooth as possible. In order to quantify the contribution of these long MFPs to the thermal conductivity, we present in Fig. 10 an histogram of the contribution to the total conductivity of the first, second, third and last quarter of the MFPs distribution. For the 3 diameters, the distribution is approximately the same : 60 to 70 % of the thermal conductivity is provided by phonon MFPs distributed from 0 to $\Lambda_{\max}/4$. Another 25 % is provided by MFPs between $\Lambda_{\max}/4$ and $3\Lambda_{\max}/4$. The longest MFPs, from $3\Lambda_{\max}/4$ to Λ_{\max} contributes to $\approx 5\%$ of the total thermal conductivity. For the thinnest NWs ($D = 3\text{nm}$), 30 % of the thermal conductivity is provided by phonon MFPs in the range [75:300] nm. This range shifts to larger values when the diameter increases : [150:500] nm for $D=10$ nm and [200:700] nm for $D=14$ nm. In conclusion, the NW-FETs acutally developed with the two latter diameters, could benefit of an improvement in the heat dissipation if the surface states is optimised, and even if the length of the NWs themselves will probably be smaller than the maximum phonon MFPs, they are generally connected to larger blocks acting for example as source/drain where these phonon large MFPs could exist.

VII. CONCLUSION

In conclusion, we systematically calculated the thermal conductivity of Si nanowires with diameters from 1 to 14 nm and lengths up to $1.2 \mu\text{m}$ by approach-to-equilibrium molecular dynamics. The temperature transient and spatial distribution comply with the time-dependent solution of the heat equation, whenever the length is equal to a few tenths of nms or several hundreds of nms. Therefore a deviation from the Fourier regime is not evidenced. A 1D thermal conductivity is obtained from the temperature transient. The length dependence of the thermal conductivity is analysed. At small length, the thermal conductivity increases when the length increases. At long length, the thermal conductivity saturates. The threshold corresponds to the maximum value of the phonon MFPs distribution. It remains as large as hundreds of nanometers in the smooth NWs studied in this work. The low-length regime corresponds to the accumulation of the phonon MFPs contributions, as observed in bulk silicon. At long length, all the MFPs are included and the thermal conductivity is fixed

at a given diameter. A divergence of the thermal conductivity is not observed.

VIII. ACKNOWLEDGEMENTS

This work was funded by the French ANR via the project n. ANR-13-NANO-0009 “NOODLES” and by Equipex EXCELSIOR (<http://www.excelsior-ncc.eu>). The computations were performed by using resources from GENCI (Grand Equipement National de Calcul Intensif) (Grant No.[2016]097600, [2015]096939, [2014]096939). Evelyne Lampin acknowledges Christophe Delerue for discussions on the 1D electrical and thermal conductivities.

-
- ¹ D. Li, Y. Wu, P. Kim, L. Shi, P. Yang and A. Majumdar, *Appl. Phys. Lett.* **83**, 2934 (2003).
 - ² C. J. Glassbrenner and G. A. Slack, *Phys. Rev.* **134**, A1058 (1964).
 - ³ C.W. Chang, D. Okawa, H. Garcia, A. Majumdar, A. Zettl, *Phys. Rev. Lett.* **101**, 075903 (2008)
 - ⁴ T.-K. Hsiao, H.-K. Chang, S.-C. Liou, M.-W. Chu, S.-C. Lee and C.-W. Chang, *Nature Nanotech* **8**, 534 (2013).
 - ⁵ P. K. Schelling, S. R. Phillpot and P. Keblinski, *Phys. Rev. B* **65**, 144306 (2002).
 - ⁶ A. S. Henry and G. Chen, *J. Comput. Theo. Nanoscience* **5**, 1 (2008).
 - ⁷ D. P. Sellan, E. S. Landry, J. E. Turney, A. J. H. McGaughey and C. H. Amon, *Phys. Rev. B* **81**, 214305 (2010).
 - ⁸ N. Yang, G. Zhang and B. Li, *Nano Today* **5**, 85 (2010).
 - ⁹ X. Yang, A. C. To and R. Tian, *Nanotechnology* **21**, 155704 (2010).
 - ¹⁰ M. Hu, X. Zhang, K. P. Giapis and D. Poulikakos, *Phys. Rev. B* **84**, 085442 (2011).
 - ¹¹ E. Lampin, Q. H. Nguyen, P.-A. Francioso and F. Cleri, *Appl. Phys. Lett.* **100**, 131906 (2012).
 - ¹² E. Lampin, P. L. Palla, P.-A. Francioso and F. Cleri, *J. Appl. Phys.* **114**, 033525 (2013).
 - ¹³ H. Zaoui, P. L. Palla, F. Cleri and E. Lampin, Length dependence of thermal conductivity by approach-to-equilibrium molecular dynamics, *Phys. Rev. B* **94**, 054304.
 - ¹⁴ Y. Cui, Z. Zhong, D. Wang W. U. Wang, and C. M. Lieber, *NanoLett.* **3**, 149 (2003).
 - ¹⁵ T. Ernst, L. Duraffourg, C. Dupre, E. Bernard, P. Andreucci, S. Becu, E. Ollier, A. Hubert et al., *Proc. IEEE Int. Electron Device Meeting*, p. 745 (2008).
 - ¹⁶ J. Tersoff, *Phys. Rev. B* **38**, 9902 (1988).

- ¹⁷ E. Lampin, P. L. Palla, H. Zaoui and F. Cleri, Chapter: Approach-to-equilibrium molecular dynamics, in *Amorphisation and thermal properties of semiconductors: From bulk to nanostructures*, ed. K. Termentzidis, Pan Stanford (in press).
- ¹⁸ But the temperature difference is kept to 200 K in most of the simulations since the larger the initial temperature difference, the larger the amplitude of the decay signal to fit.
- ¹⁹ S. D. Suk , M. Li , Y. Y. Yeoh , K. H. Yeo , K. H. Cho , I. K. Ku , H. Cho , W. Jang , D.-W. Kim , D. Park and W.-S. Lee, IEDM Tech. Dig., pp. 891-894 (2007).
- ²⁰ R. Ng , T. Wang , F. Liu , X. Zuo , J. He and M. Chan, IEEE Electron Device Lett., **30**, 520 (2009).
- ²¹ T. Hiramoto , J. Chen and T. Saraya, Proc. 10th IEEE ICSICT, pp. 9-12 (2010).
- ²² M. Koyama, M. Cass, R. Coquand, S. Barraud, G. Ghibaudo, H. Iwai and G. Reimbold, Proc. of the European solid-State Device Research Conference pp 300-303 (2013). DOI: 10.1109/ESSDERC.2013.6818878
- ²³ J. Goldberger, A. I. Hochbaum, R. Fan and P. Yang, NanoLett. **6**, 973 (2006).
- ²⁴ K. Trivedi, H. Yuk, H. C. Floresca, M. J. Kim and W. Hu, NanoLett. **11**, 1412 (2011).
- ²⁵ J. Zou and A. Balandin, J. Appl. Phys. **89**, 2932 (2001).
- ²⁶ I. Ponomareva, D. Srivastava and M. Menon, NanoLett. **7**, 1155 (2007).
- ²⁷ F. H. Stillinger and T. A. Weber, Phys. Rev. B **31**, 5262 (1985).
- ²⁸ D. Donadio and G. Galli, NanoLett. **10**, 847 (2010).
- ²⁹ Y. He and G. Galli, Phys. Rev. Lett. **108**, 215901 (2012).

Figures



FIG. 1: Atomic structure of a crystalline silicon nanowire with $D=10$ nm and $L=200$ nm.

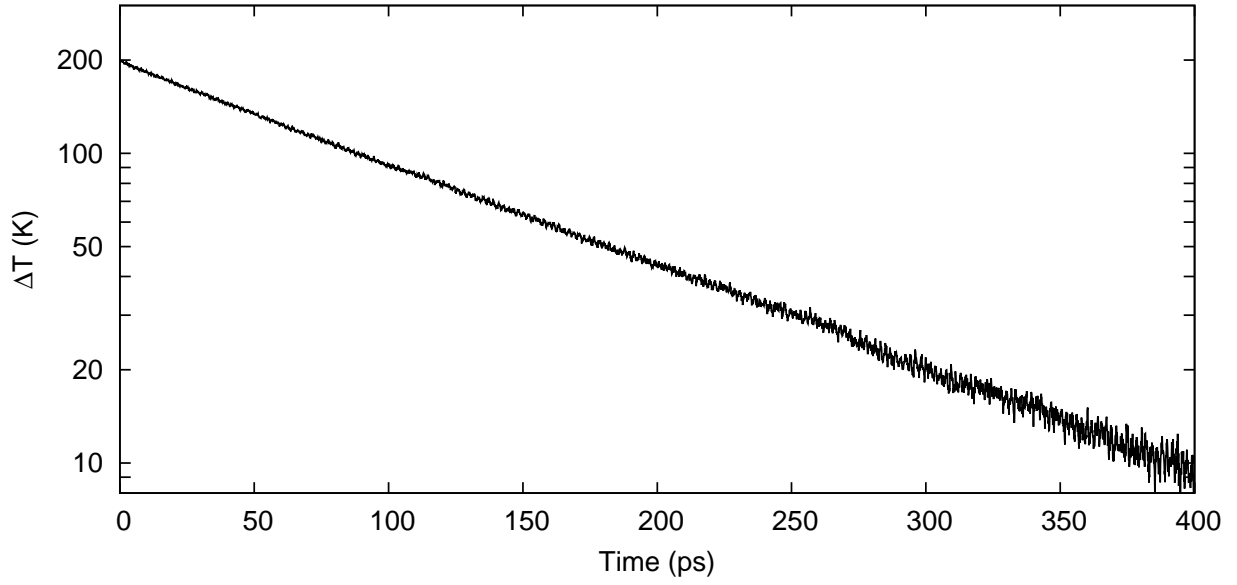


FIG. 2: Temperature difference between the hot and cold blocks during the approach-to-equilibrium. $D=10$ nm and $L = 200$ nm.



FIG. 3: Schematics of the NW of finite length L periodised along z . φ_i and φ_o are the inward and outward thermal currents.

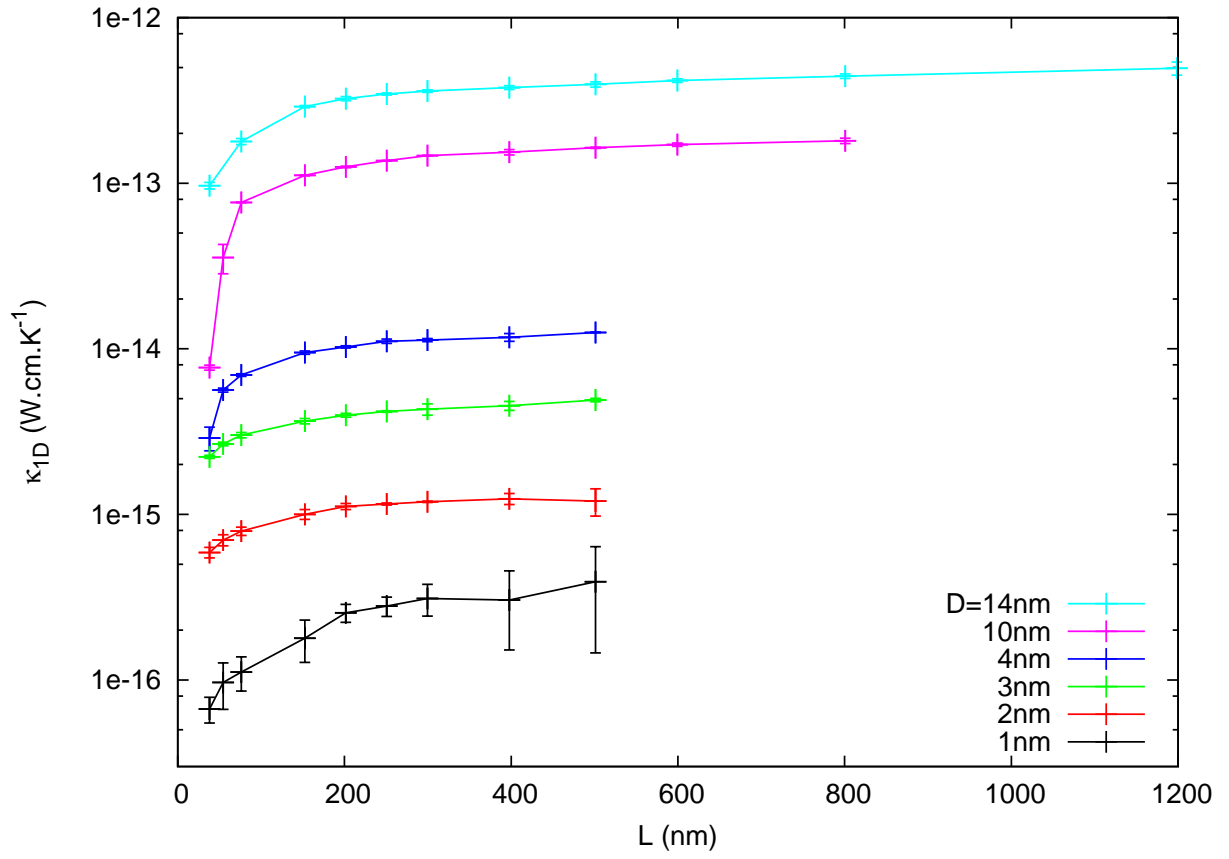


FIG. 4: NW 1D thermal conductivity κ_{1D} versus length L and for diameter D from 1 to 14 nm.

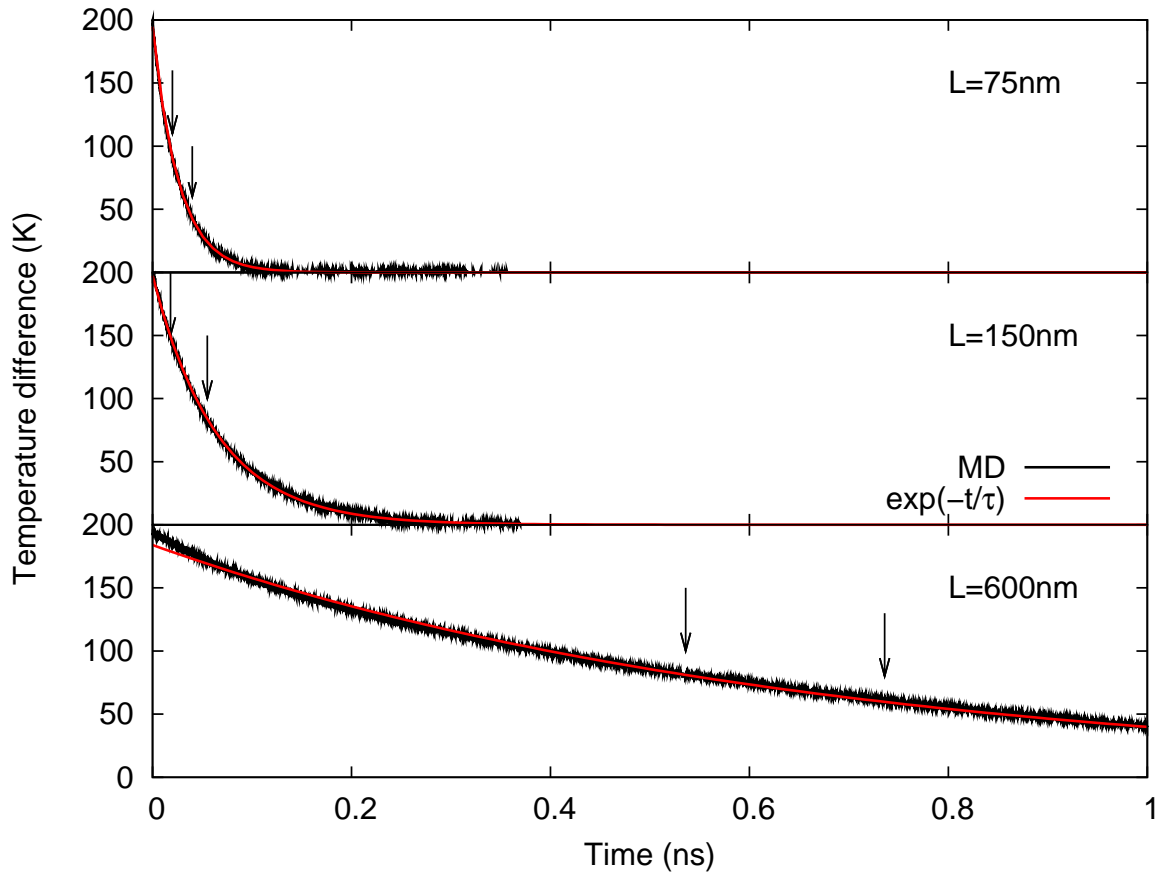


FIG. 5: Temperature difference between the hot and cold blocks during the approach-to-equilibrium for the thickest nanowire ($D=14$ nm) and three lengths ($L=75$, 150 and 600 nm). The dark lines are the MD results. The red lines are exponential decay adjusted on the MD results.

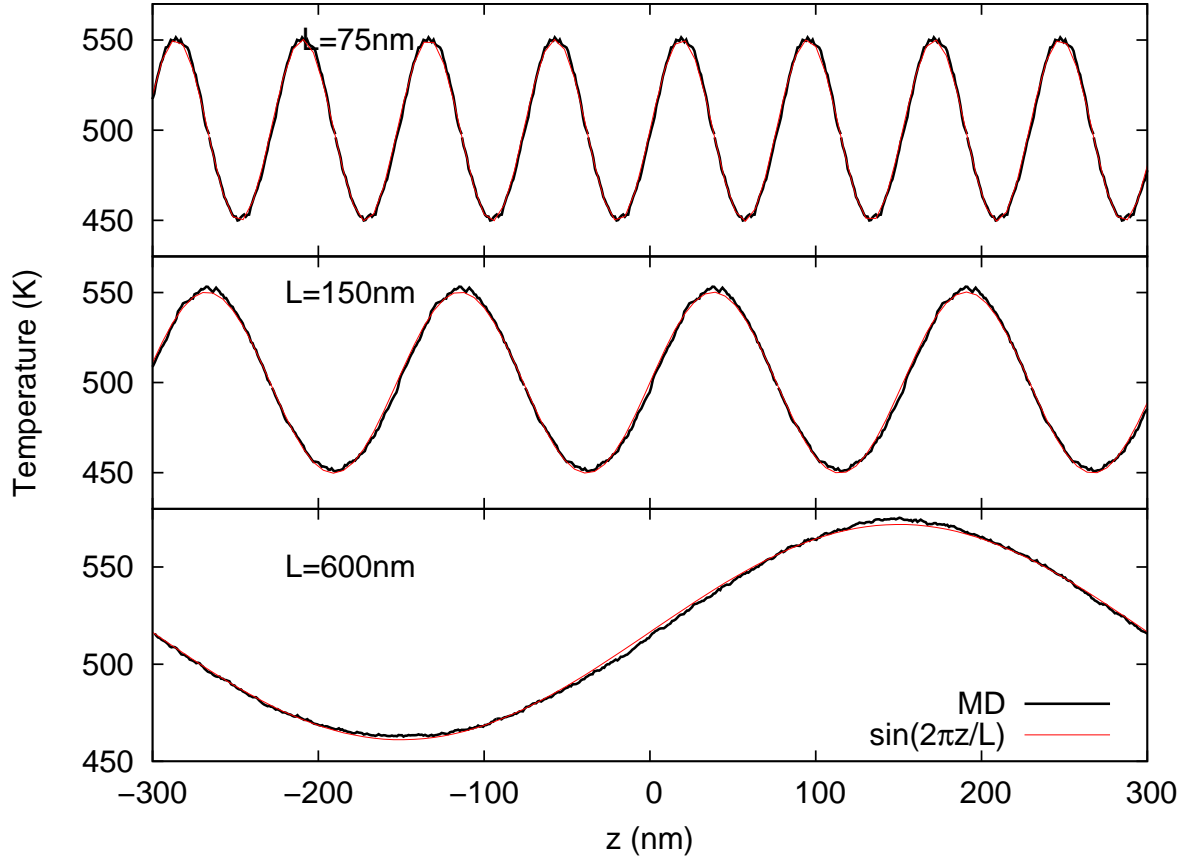


FIG. 6: Temperature profiles in nanowires of diameter $D=14$ nm and length $L=75$, 150 and 600 nm. The dark lines are the MD results. The red lines are sine curves adjusted on the MD results.

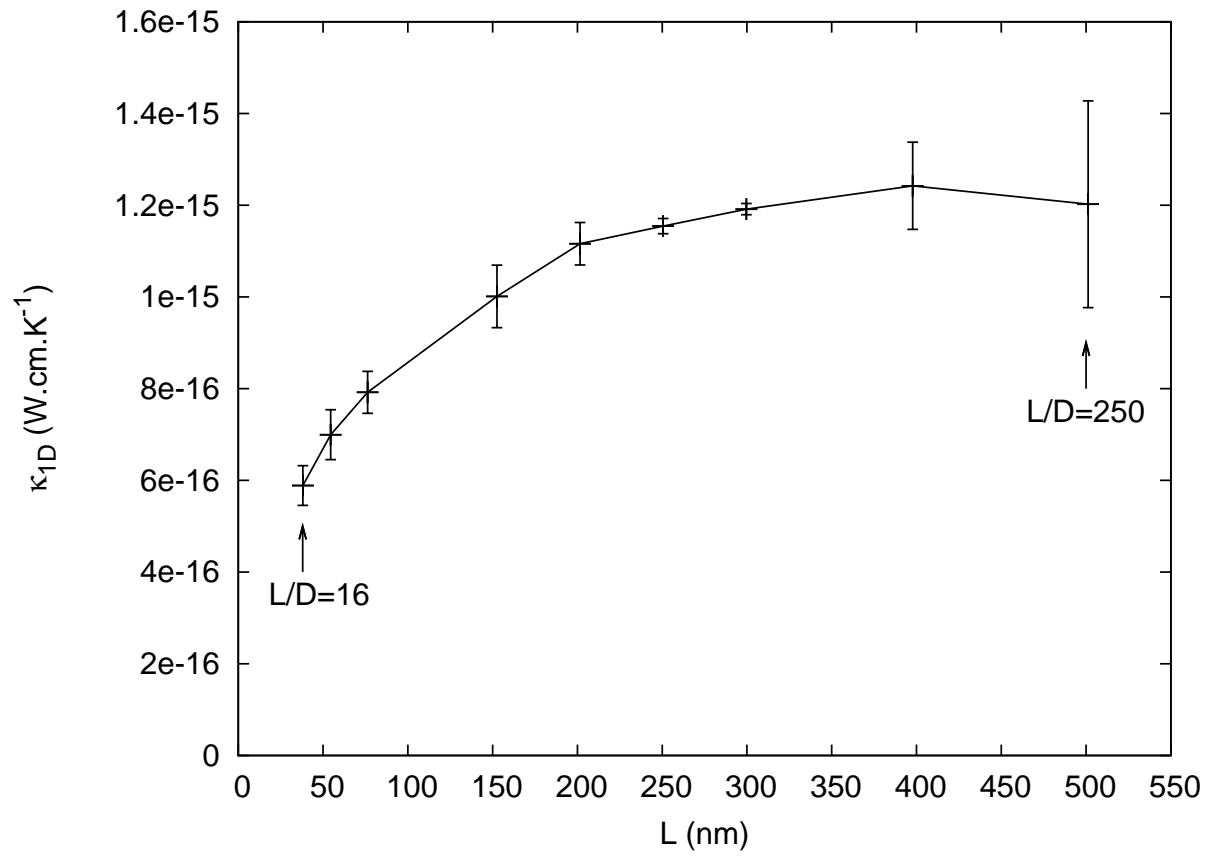


FIG. 7: 1D thermal conductivity of the $D=2\text{nm}$ nanowire versus length L .

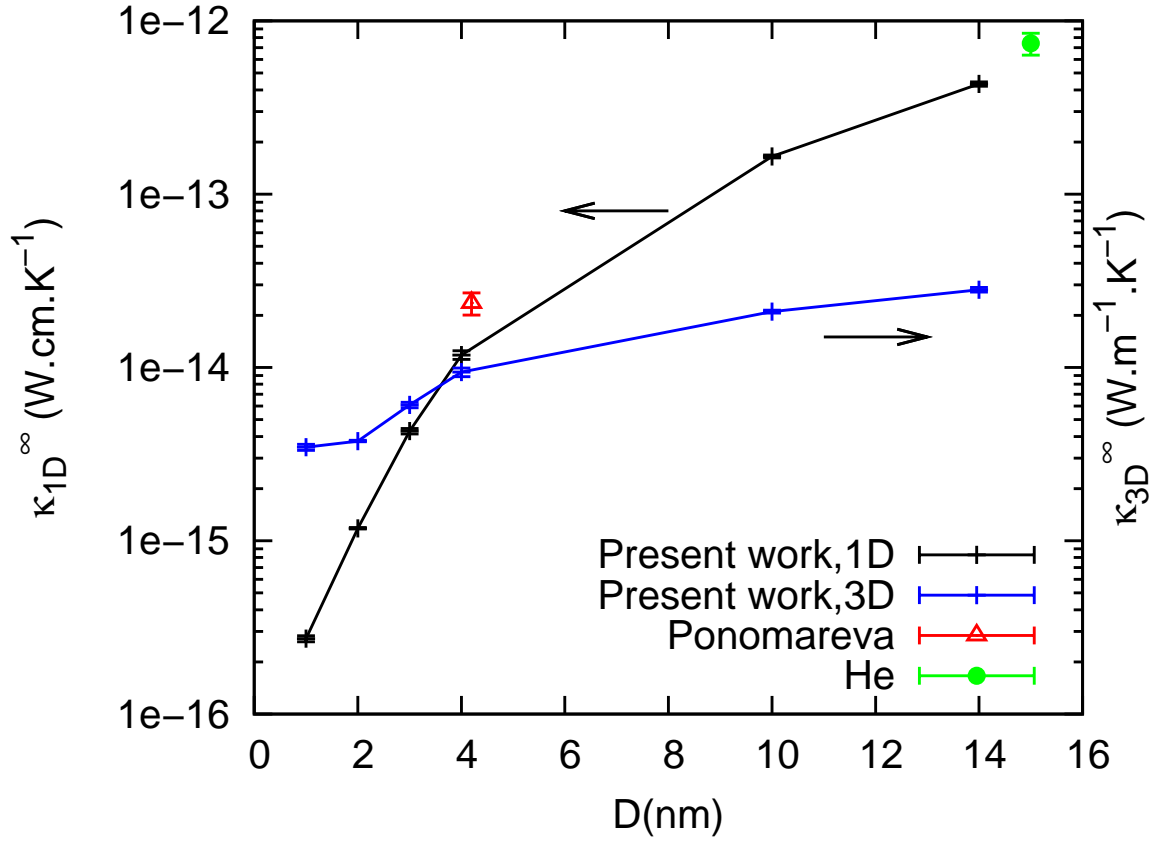


FIG. 8: NW 1D and 3D thermal conductivity at saturation versus diameter (black points). In red, the calculation from Ponomareva et al.²⁶ In green the calculation from He et al.²⁹ The two latter, obtained in $\text{W.m}^{-1}.\text{K}^{-1}$ by the authors, have been converted to 1D thermal conductivities using the cross section.

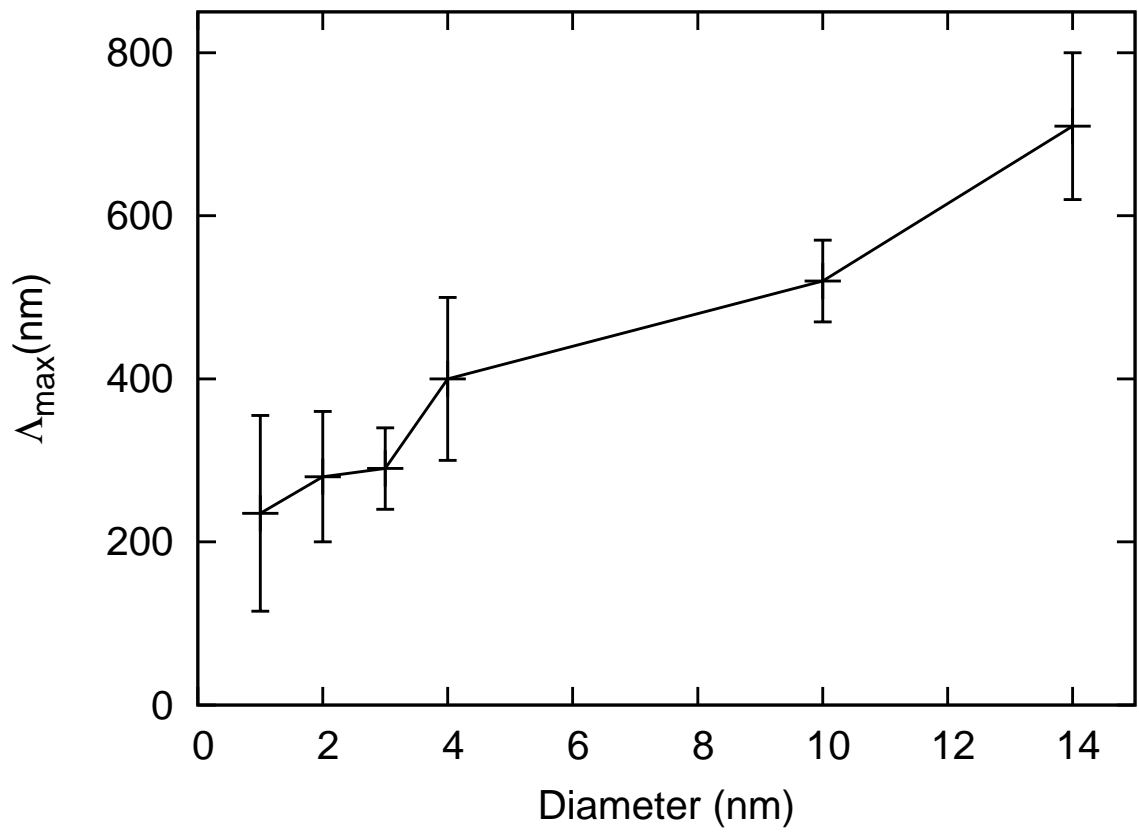


FIG. 9: Maximum phonon mean free path versus NW diameter.

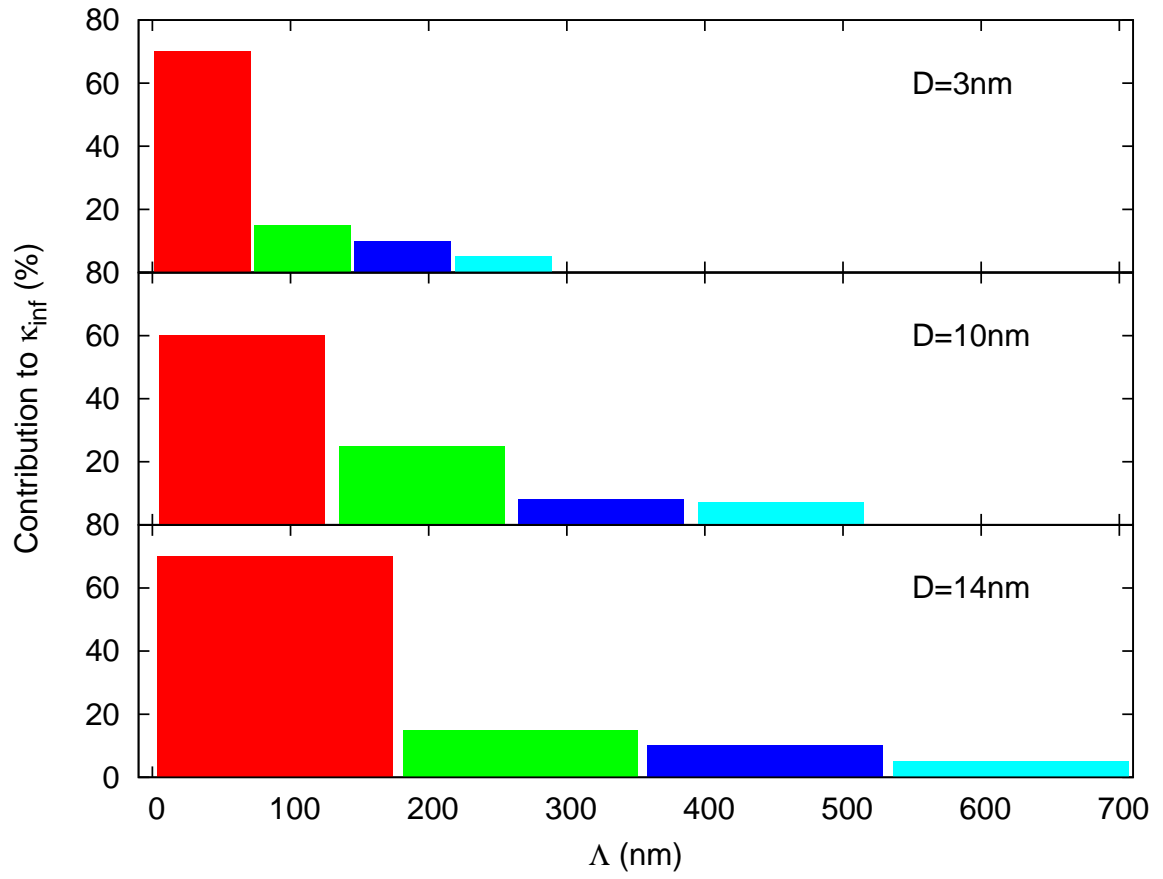


FIG. 10: Contribution to thermal conductivity versus the phonon MFP range for the NWs of diameter equal to $D=3$, 10 and 14 nm.